PERGAMON

Carbon 39 (2001) 615–628

CARBON

Letters to the editor

Graphite–graphite electrical contact under dynamic mechanical loading

Xiangcheng Luo, D.D.L. Chung*

Composite Materials Research Laboratory, State University of New York at Buffalo, Buffalo, NY 14260-4400, USA

Received 5 February 2000; accepted 4 September 2000

Keywords: A. Synthetic graphite; D. Electrical properties; Mechanical properties

Due to its electrical conductivity, thermal conductivity, oxidation resistance and wear resistance, graphite is used as an electrical contact material, particularly in sliding conditions, as encountered by brushes for electric motors and other devices and by sliding electrical contacts for trams and other electric vehicles [1–8]. To further improve the conductivity, copper impregnated graphite may be used [9,10]. Because of this application, the quality of graphite–graphite electrical contacts over time under dynamic mechanical loading is of interest. Relevant questions concern how elastic and plastic deformations at the contact interface (particularly at the asperities) affect the quality of the electrical contact under mechanically loaded and unloaded conditions, and how these effects depend on the stress amplitude and the number of loading cycles.

Wear or abrasion involves subjecting each point of a surface to dynamic shear. Studies of wear or abrasion are commonly conducted by monitoring the effect over an area rather than that at a fixed point. For example, in wear testing using the pin-on-disk configuration, the tip of the pin is continuously moved against the surface of the disk, so that different points on the disk are subjected to stress at different times and the effect of dynamic shear and the stress variation within a cycle of dynamic shear at a particular point of the surface are not monitored. Even if the effect of wear or abrasion is monitored in real time, say by measuring the contact electrical resistance at the sliding contact between the pin and the disk, the monitoring does not allow correlation of the effect (say the electrical resistance) at a point with the dynamic stress at the point within a stress cycle. (The dynamic stress is to be distinguished from the stress amplitude.) This difficulty with wear or abrasion studies stems from the fact that wear or abrasion involves one element sliding against another, so that different points in a contact are not subjected to dynamic stress in an in-phase manner. In contrast, dynamic compression does not involve sliding, so that each point in a contact is subjected to dynamic compression in an in-phase manner, i.e. all points experience the maximum compressive stress in a cycle simultaneously and all points experience the minimum stress in a cycle simultaneously. As a result, correlation is possible between the effect (say the contact electrical resistance at the contact) and the dynamic stress during dynamic loading. This correlation allows identification of the point in a stress cycle at which certain effect occurs, and moreover allows distinction between reversible effects (such as elastic deformation, which vanish upon unloading) and irreversible effects (such as plastic deformation, which remain upon unloading). Therefore, by studying the effect of dynamic compression rather than dynamic shear, this paper provides new information on the dynamic mechanical behavior of contacts, i.e. the behavior of contacts under dynamic loading.

The technique used in this work for studying the dynamic mechanical behavior of contacts is contact electrical resistance measurement during dynamic compression below the yield stress. It involves simultaneous electrical and mechanical measurements. The technique requires that the elements in contact are electrically conducting. The contact resistance of the interface between contacting elements can be conveniently measured by using the elements as electrical leads — two for passing current and two for voltage measurement (i.e. the four-probe method), as provided by two elements (beams) that overlap at 90° (Fig. 1). The volume resistance of each lead was negligible compared to the contact resistance of the junction, so the measured resistance (i.e. voltage divided by current) was

*Corresponding author. Tel.: +1-716-645-2593; fax: +1-716-645-3875.

E-mail address: ddlchung@acsu.buffalo.edu (D.D.L. Chung).

0008-6223/01/$ – see front matter
PII: S0008-6223(00)00262-1

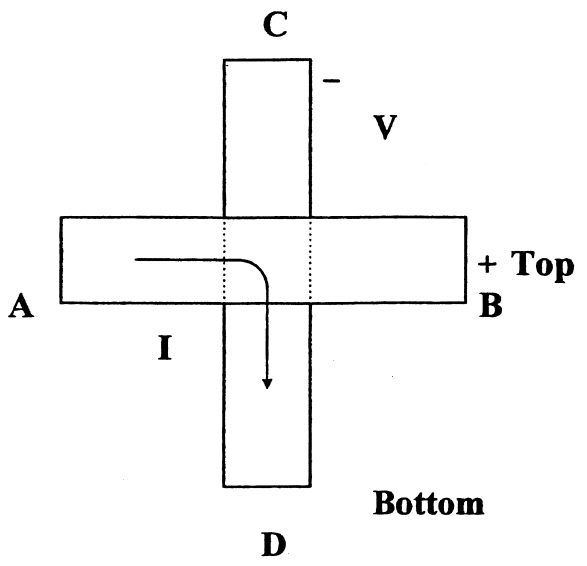

Fig. 1. Sample configuration for contact electrical resistance measurement.

the contact resistance. The contact resistance multiplied by the junction area gives the contact resistivity, which is independent of the junction area and describes the structure of the interface.

Contact electrical resistance measurement has been previously used to study the interface between laminae in a carbon fiber polymer-matrix composite laminate [11] and to study the joint obtained between thermoplastic elements by autohesion [12,13]. In the field of concrete, contact electrical resistance measurement has been previously used to study the joint between old and new concrete [14], as this joint is relevant to the repair of concrete structures. It has also been used to study the interface between concrete and steel [15,16] and that between cement paste and carbon fiber [17,18].

The material used in this work is electrographitic carbon of Grade EG389P (from Carbone of America Corp., Boonton, NJ). The flexural strength is 16.5 MPa, according to the manufacturer. The compressive strength is 32.6 MPa and the 0.2%-offset yield strength is 25.8 MPa, as measured in this work by compression testing using a rectangular sample of size 11.8×11.1 mm perpendicular to the stress direction and 12.9 mm in the stress direction and using an attached strain gauge for measuring the strain in the stress direction. The electrical resistivity is 2×10^{-3} Ω cm, the density is 1.46 g/cm^3, and the shore hardness is 30, according to the manufacturer.

The graphite was cut into rectangular strips of length 7.9–8.2 mm, width 7.0–7.8 mm and thickness 4.2 mm using a diamond saw. The surfaces of the strips were mechanically polished using 600-grit sandpaper, followed by washing with flowing water for the purpose of cleaning. Two strips were allowed to overlap at 90° to form a nearly square junction of size 7.9–8.2 mm by 7.0–7.8 mm, as illustrated in Fig. 1. The junction was the joint under study. After mechanical testing at each compressive stress amplitude (as described below), the sample surfaces were polished and cleaned again, so that testing at each stress amplitude was conducted on freshly prepared surfaces.

Uniaxial dynamic compression was applied at the junction in the direction perpendicular to the junction, using a screw-action mechanical testing system (Sintech 2/D, Sintech, Research Triangle Park, NC), while the contact electrical resistance of the junction was measured using a Keithley 2002 multimeter. Copper wires were applied around the strips together with silver paint to serve as electrical contacts. A DC current was applied from A to D (Fig. 1), so that the current traveled down the junction from the top strip to the bottom strip. The use of two current probes (A and D) and two voltage probes (B and C) corresponded to the four-probe method of resistance measurement. The voltage divided by the current yielded the contact resistance of the junction. The crosshead displacement during load cycling was typically up to 6 μm.

Fig. 2 shows the variation of the contact resistance with stress during cyclic compressive loading at a stress amplitude of 0.35 MPa. In every cycle, the resistance decreased as the compressive stress increased, such that the maximum stress corresponded to the minimum resistance and the minimum stress corresponded to the maximum resistance. During cycling, the minimum resistance (at the maximum stress) remained at the same level and the maximum resistance (at zero stress) did not show any systematic change. Since graphite essentially does not undergo oxidation at room temperature, the contact resistance variation is attributed to the change in contact area.

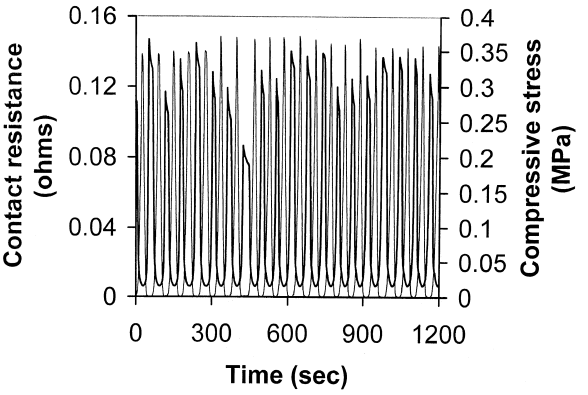

Fig. 2. Variation of contact resistance with time and of compressive stress with time during cycling compression at a stress amplitude of 0.35 MPa.

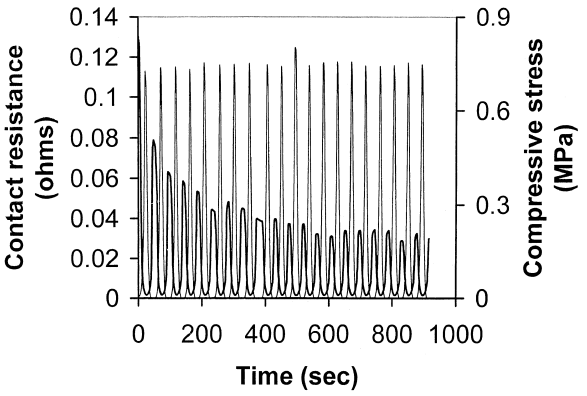

Fig. 3. Variation of contact resistance with time and of compressive stress with time during cycling compression at a stress amplitude of 0.70 MPa.

Upon compressive loading, more contact area was created, thus the contact resistance decreased; upon unloading, the reverse occurred. This means that, at this stress amplitude, elastic deformation dominated the overall deformation. Although the stress at the surface asperities could be higher than the yield stress of graphite, no significant plastic deformation on the surface occurred. The contact resistance ranged from 0.007 to 0.12 Ω.

The stress amplitude in Fig. 3 is 0.7 MPa, which is higher than that in Fig. 2. The resistance changed similarly at the two stress amplitudes, except that, in Fig. 3, the contact resistance at zero stress decreased gradually upon cycling for about 11 cycles before leveling off. The leveled-off resistance ranged from 0.002 to 0.030 Ω.

Fig. 4 shows the contact resistance change at the stress amplitude of 1.4 MPa. The resistance at zero stress essentially took only the first cycle to level off. The

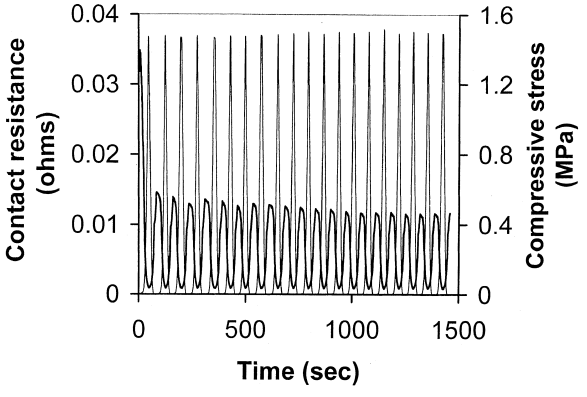

Fig. 4. Variation of contact resistance with time and of compressive stress with time during cycling compression at a stress amplitude of 1.4 MPa.

leveled-off contact resistance ranged from 0.001 to 0.013 Ω.

The highest stress amplitude of 1.4 MPa (much lower than the yield strength, 25.8 MPa) corresponded to a strain of 0.14%, according to the compressive stress–strain curve. For the sample thickness (4.2 mm) used for measuring the contact electrical resistance, this strain corresponded to a dimensional change (shrinkage) of 6 μm. Thus, the displacement associated with Figs. 2–4 is negligible.

Although the stress amplitudes used were all much below the yield strength, the local stress at asperities could be high enough to cause plastic deformation. The decrease of the contact resistance at zero stress in Figs. 3 and 4 is attributed to the plastic deformation at the asperities during loading. When the stress was removed, the contact area at asperities did not return to the initial value. In Fig. 3 the gradual decrease means that plastic deformation occurred progressively upon cycling, due to the intermediate level of the stress amplitude; in Fig. 4 the abrupt decrease means that plastic deformation essentially occurred only in the first loading cycle, due to the higher stress amplitude. The leveling off of the resistance is attributed to the attainment of the maximum amount of plastic deformation at the corresponding stress amplitude. The higher the stress amplitude, the smaller was the leveled off resistance and the smaller were the contact resistances at maximum and zero stresses; the higher the applied stress, the smoother was the surface upon loading, the less was the room for the contact area to be further decreased by loading, and the more was the contact area at maximum or zero stress.

The resistance at the maximum stress remained the same upon cycling at all three stress amplitudes; so did the shape of the resistance vs. time curve of a cycle. This is due to the dominance of elastic deformation in the loaded state.

The results reported here were obtained for the particular grade of electrographitic carbon and the particular surface finish used. As the degree of graphitization, mechanical properties and surface finish vary widely among carbons used for brushes in electric motors, the results reported here should not be assumed to apply to all types of carbons.

In summary, a graphite–graphite contact was studied by measuring the contact electrical resistance during compressive cyclic loading. The contact resistance decreased quite reversibly upon loading, due to the dominance of elastic deformation. The contact resistance at the maximum stress remained the same upon cycling at any of the three stress amplitudes used. A decrease of the contact resistance at zero stress occurred upon cycling at stress amplitudes of 0.70 and 1.40 MPa, but did not occur at the lowest stress amplitude of 0.35 MPa. The decrease of the resistance at zero stress upon cycling is due to local plastic deformation at the asperities. The higher the stress amplitude, the fewer was the number of cycles for the resistance to level off.

The higher the stress amplitude, the lower was the contact resistance both at maximum and zero stresses.

References

[1] Shobert EI. In: Carbon brushes: the physics and chemistry of sliding contacts, New York, NY: Chemical Publishing, 1965, pp. 185–6.

[2] Hounkponou E, Nery H, Paulmier D, Bouchoucha A, Zaidi H. Tribological behavior of graphite/graphite and graphite/copper couples in sliding electrical contact: influence of the contact electric field on the surface passivation. Appl Surf Sci 1993;70–71(1–4):176–9.

[3] Duthie FW. Long life brushes — 100 years. In: Coil Winding Proceedings, Minneapolis, MN: International Coil Winding Association, 1985, pp. 65–76.

[4] Rabinowicz E, Ross AZ. Compatibility effects in the sliding of graphite and silver-graphite brushes against various ring materials. In: Electrical Contacts — 1984: Proceedings of the Twelfth International Conference on Electric Contact Phenomena, Meeting Jointly with the Thirtieth Annual Holm Conference on Electrical Contacts, Illinois Institute of Technology, Chicago, IL, 1984, pp. 499–506.

[5] Konchits VV. Frictional interaction and current passage in composite–metal sliding electrical contact — II. Soviet J Friction Wear 1984;5(1):44–9, (English translation of Trenie i Iznos).

[6] Milkovic M, Ban D. Influence of the pulsating current amplitude on the dynamic friction coefficient of electrographite brushes. Carbon 1996;34(10):1207–14.

[7] Bryant MD, Burton RA. Frictional and electrical interactions in current collectors. Wear 1982;78((1,2)), Adv Curr Collect Conf, Chicago, IL, 1981;Sep. 23–25:49–58.

[8] Wu Y, Zhang G, Tang W. Research of fiber/graphite composite brush. In: Electrical Contacts, Proceedings of the 41st IEEE Holm Conference on Electrical Contacts, Piscataway, NJ: IEEE, 1995, pp. 315–22.

[9] Lu C-T, Bryant MD. Simulation of a carbon graphite brush with distributed metal particles. IEEE Trans Components Packag Manuf Technol Part A 1994;17(1):68–77.

[10] Dillich S, Kuhlmann-Wilsdorf D. Two regimes of current conduction in metal–graphite electrical brushes and resulting instabilities. IEEE Trans Components Hybrids Manuf Technol 1983;1:45–54.

[11] Wang S, Chung DDL. Interlaminar interface in carbon fiber polymer–matrix composites. Studied by contact electrical resistivity measurement. Composite Interfaces 1999;6(6):497–506.

[12] Mei Z, Chung DDL. Kinetics of autohesion of thermoplastic carbon-fiber prepregs. Int J Adhesion and Adhesives 2000;20:173–5.

[13] Mei Z, Chung DDL. Thermal stress induced thermoplastic composite debonding. Studied by contact electrical resistance measurement. Int J Adhesion and Adhesives 2000;20:135–9.

[14] Chen P-W, Fu X, Chung DDL. Improving the bonding between old and new concrete by the addition of carbon fibers to the new concrete. Cem Concr Res 1995;25(3):491–6.

[15] Fu X, Chung DDL. Bond strength and contact electrical resistivity between cement and stainless steel fiber: their correlation and dependence on fiber surface treatment and curing age. ACI Mater J 1997;94(3):203–8.

[16] Fu X, Chung DDL. Effects of water–cement ratio, curing age, silica fume, polymer admixtures, steel surface treatments, and corrosion on bond between concrete and steel reinforcing bars. ACI Mater J 1998;95(6):725–34.

[17] Fu X, Lu W, Chung DDL. Improving the bond strength between carbon fiber and cement by fiber surface treatment and polymer addition to cement mix. Cem Concrete Res 1996;26(7):1007–12.

[18] Fu X, Chung DDL. Contact electrical resistivity between cement and carbon fiber: its decrease with increasing bond strength and its increase during fiber pull-out. Cem Concrete Res 1995;25(7):1391–6.

Carbon nanocells grown in hydrothermal fluids

Jose Maria Calderon Moreno*, Takahiro Fujino, Masahiro Yoshimura

Materials and Structures Laboratory, Tokyo Institute of Technology, 4259 Nagatsuta, Midori-ku, Yokohama 226-8503, Japan

Received 24 June 2000; accepted 21 October 2000

Keywords: A. Amorphous carbon; B. Hydrothermal treatment; C. Transmission electron microscopy, Raman spectroscopy; D. Microstructure

The discovery, synthesis and characterization of nanocarbon structures: fullerenes, nanotubes and nanofibers, has received much attention due to their unique crystal structure and properties. Nano-structured carbons have potential applications as high strength reinforcing materials, lubricants, point field emitters, nanowires [1], etc. The existence of other forms of finite nanocarbons has also attracted great interest. The formation of well ordered structures made of graphitic layers arranged concentrically has been reported in very high-temperature or high-energy input

*Corresponding author. Tel.: +81-0-45-924-5323; fax: +81-0-45-924-5358.

E-mail address: calderon1@rlem.titech.ac.jp (J.M.C. Moreno).

0008-6223/01/$ – see front matter
PII: S0008-6223(00)00283-9